



## Advances in Scanning Tunneling Microscopy: Principles, Capabilities, and Impact on Nanotechnology

**Dr. Anupam Debangshi**

*Assistant Professor, Surendranath Evening College, Kolkata*

ORCID: [0000-0002-4627-6673](https://orcid.org/0000-0002-4627-6673)

### **Abstract**

*This study explains STM theory and tunneling principles while evaluating an STS-based research paper, emphasizing its methods, findings, and significance in understanding surface structure and electronic properties at the nanoscale. Human is curious by nature and that leads him to explore the enormous mysteries of the universe. The journey of knowledge has started from the very early days of the human civilization. Scientists have invented various tools to study their desirables outstretched between the cosmos and the subatomic realm. One of the edge cutting invention is the Scanning Tunneling Microscope (STM) which is developed by Gerd Binnig and Heinrich Rohrer in the early period of 1980s in the IBM research laboratory, Zürich. This revolutionary invention has provided the insight to the subatomic world which is beyond our optical vision. This miracle instrument can provide a real space image at subatomic level and also can manipulate individual atoms and molecules. Very local detailing of molecules such as surface defects, electrical properties, band structure and many more properties can be obtained using this device. In the year of 1986 Gerd Binnig and Heinrich Rohrer have been honored with the most prestigious the Noble prize for this groundbreaking invention.*

**Keywords:** STM, Scanning Tunneling Microscopy, Nanotechnology, Tunneling

### **Introduction**

The scanning tunneling microscope (STM), is a landmark achievement in surface science and a foundational tool in the emergence of nanotechnology. Operating on the principle of quantum tunneling, the STM uses a finely sharpened conductive tip brought within a few angstroms of a sample surface. When a small bias voltage is applied, electrons tunnel across the minuscule gap between the tip and the surface, producing a tunneling current that is extremely sensitive to changes in distance. By maintaining or monitoring this current as the tip scans across the surface, the STM generates three-dimensional images with true atomic resolution, revealing not only the positions of individual atoms but also variations in electronic density and local surface features.

The objective of this work is to explain the basic theory of Scanning Tunneling Microscopy, emphasizing its reliance on quantum tunneling between a sharp tip and conductive surface. It also aims to describe the tunneling mechanism governing current variations with tip-sample separation. Additionally, the study discusses a selected research paper using Scanning Tunneling Spectroscopy, highlighting its methodology, key findings, and significance in analyzing local electronic states of materials.

The significance of the STM extends far beyond high-resolution imaging. It introduced the possibility of direct atomic manipulation, as demonstrated when researchers used it to position individual atoms to form predetermined patterns, a milestone that showcased the ability to construct structures atom by atom. This capability fundamentally reshaped the understanding of material behavior at the nanoscale and provided a practical

tool for probing interactions, chemical bonding, and quantum effects in unprecedented detail. The STM also enabled the investigation of surface phenomena such as adsorption, diffusion, and reconstruction, which play critical roles in catalysis, semiconductor technology, and materials engineering.

In nanotechnology, the STM has been indispensable for characterizing nanomaterials including thin films, nanowires, quantum dots, and molecular assemblies. Its ability to map electronic states allows scientists to explore quantum confinement, superconductivity, and charge transport at the level of individual atoms or molecules. Furthermore, the conceptual framework of the STM inspired the development of a broader family of scanning probe microscopes, most notably the atomic force microscope (AFM), greatly expanding the range of materials that can be studied with nanoscale precision.

Overall, the STM revolutionized the study of surfaces and initiated a paradigm shift in how matter can be observed and engineered. By enabling both visualization and manipulation at the atomic scale, it laid the scientific and technological foundations for modern nanotechnology, influencing everything from fundamental physics to advanced material design and nanoscale device fabrication.

## Principles of Scanning Tunneling Microscope:

The quantum mechanical tunneling of electrons is the main working principle of STM. In STM two metal electrodes (tip and substrate) are separated by a vacuum potential barrier ( $V$ ). Classically, the electron can overcome the potential barrier when its energy ( $E$ ) is larger than the height of the barrier ( $E > V$ ), but if the electron energy is smaller than the barrier height ( $E < V$ ), the electron can't pass through it. In quantum mechanics the electron propagation mechanism is somehow different. According to wave particle duality electron can pass through the higher potential barrier as it has the finite tunneling probability across the barrier (Figure 1). The tunneling probability of electron is dependent on barrier height and width, which can be calculated from the Schrödinger equation. Inside the metal electrode  $\Psi(z)$  is a wave function of electron which is a complex exponential function (Figure 1), but at the surface the corresponding electron wave function decays exponentially

into the vacuum  $\psi(z) = \psi(0)e^{-kz}$  where,  $k = \frac{\sqrt{2m_e(V-E)}}{\hbar}$  and ' $m_e$ ' is the mass of electron, ' $V$ ' is the height of the potential barrier, and ' $E$ ' is the energy of the electron<sup>1-3</sup>. Thus the tunneling current ' $I$ ', is exponentially dependent on the barrier height ( $V$ ) and width ( $z$ ). Hence, the tunneling current is extremely sensitive to the barrier height and width. In other words, there is a finite non-zero probability (square of wave function) to find an electron in the vacuum between the two metal electrodes. At zero bias voltages the Fermi levels of both the electrodes are normalized to the averaged value but when external bias voltage is applied, the Fermi levels of both metals become mutually shifted. More precisely, the electrons tunnel from filled states of one metal electrode to the empty states of other metal electrode. There are three different tunneling mechanisms probable while measuring the I-V and dI/dV properties in STM. The detailed overview of the tunneling mechanisms is depicted in the following sub-sections.

**Direct tunneling: The low bias voltage case** Figure 2 shows the Fermi level alignment of STM tip and sample in tunneling contact in zero, and with applied positive and negative bias. The difference between the Fermi energy ( $E_F$ ) and vacuum level is the work function. In equilibrium, the net tunneling current is zero (Figure 2(a)). Applied bias voltage  $V$  will shift the Fermi level by  $eV$ . At negative bias voltage  $-V$ , electrons can tunnel in the energy interval  $E_F - eV$  to  $E_F$ , into unoccupied states of the tip from the sample (Figure 2(b)). For positive bias voltage  $+V$ , the electrons tunnel from occupied states of the tip to unoccupied states of the sample (Figure 2(c)).

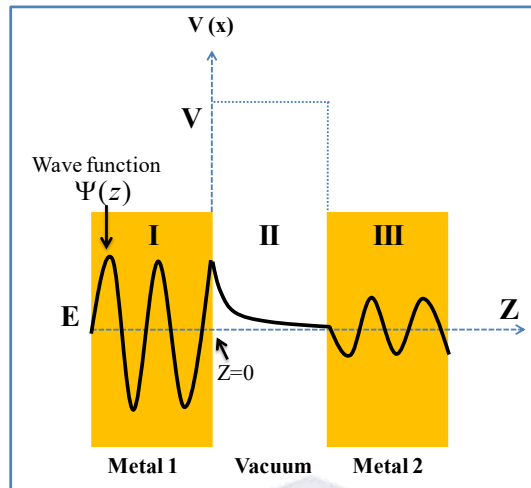


**Figure 1:** Schematic representation of the tunneling effect of electrons between two metal electrodes (metal 1 and metal 2) separated by a vacuum barrier when an electron (wave) hits a vacuum barrier of width  $z$  and height  $V$  (region I). The wave function of electron is an exponential decay function within the insulating vacuum barrier (region II). There exists certain probability, due to the wave like behavior of electron, to appear on the other side of the barrier (region III).

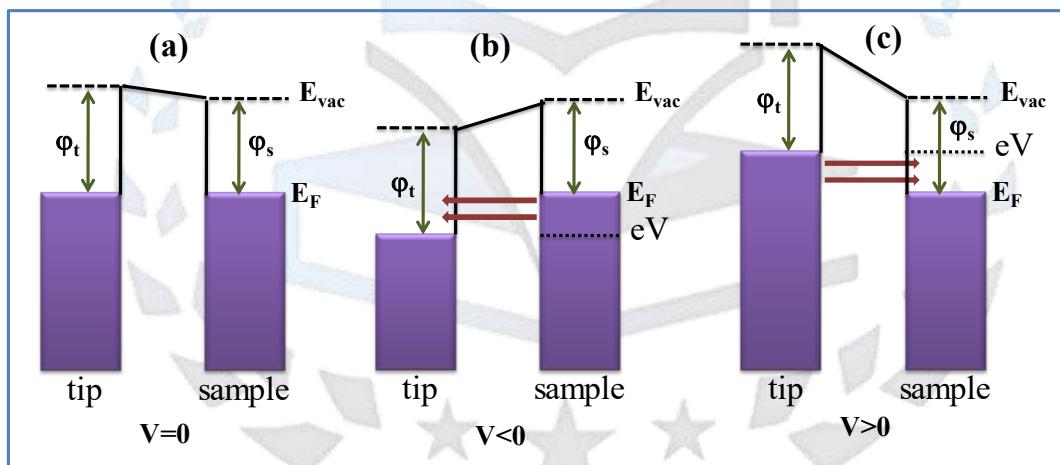


**Figure 2:** Schematic illustration of direct tunneling mechanism. Schematic showing the tunneling process of electrons between two metal electrodes: (a)  $V=0$ , no net tunneling; (b)  $V<0$ , net tunneling of electrons from sample to tip; (c)  $V>0$ , net tunneling of electrons from tip to sample.

### Fowler-Nordhiem (FN) tunneling: The high bias voltage case

Direct tunneling is the dominant charge transport process between the tip and the sample at low bias voltages (Figure 3(a)-(b)). Under Simmons approximation (trapezoidal barrier between tip and sample) the

corresponding tunneling current at zero bias is given by (Figure 3(b)),  $I \propto V \exp\left(-\frac{2d\sqrt{m_e\phi}}{\hbar}\right)$  where 'd' is

the barrier width, ' $m_e$ ' is the electron effective mass, ' $\phi$ ' is the barrier height. At the opposite limit, when the applied bias exceeds the barrier height, the barrier shape changes from trapezoidal to triangular barrier (Figure 3(c)).

The current-voltage relation at this condition can be expressed by,  $I \propto V^2 \exp\left(-\frac{4d\sqrt{2m_e\phi^3}}{3\hbar qV}\right)$  where 'q' is the

electronic charge and 'V' is the bias voltage. The tunneling mechanism through a triangular barrier at high-voltage

regime is similar to the field emission and Fowler-Nordheim (FN) tunneling. If the applied bias is equal to the barrier height, two mechanisms (FN tunneling and direct tunneling) compete, which causes a transition from logarithmic growth to linear decay. This transition point is the measure of the voltage ( $V_{\text{trans}}$ ) required changing the shape of the barrier from trapezoidal to triangular.<sup>2,3</sup>

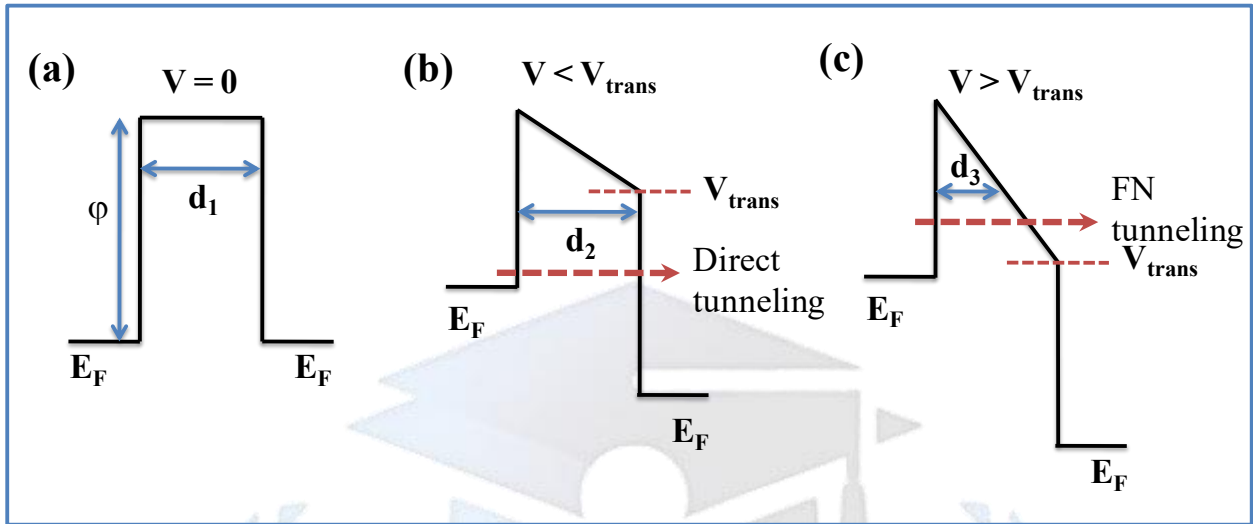


**Figure 3:** Schematic illustration of Fowler-Nordheim (FN) tunneling mechanism. (a)  $V = 0$  V, no net-tunneling of electrons occur. (b)  $V < V_{\text{trans}}$ , the electrons participate in direct tunneling through the trapezoidal barrier formed and (c)  $V > V_{\text{trans}}$ , high positive bias ( $>V_{\text{trans}}$ ) initiates the field emission of electrons through triangular region of the barrier.  $d_1$ ,  $d_2$  and  $d_3$  are the barrier widths at  $V = 0$  V,  $V < V_{\text{trans}}$  and  $V > V_{\text{trans}}$ , respectively. ' $\phi$ ' determines the height of the barrier. Horizontal dashed arrow is the tunneling path for the electrons. Horizontal dashed line represents  $V_{\text{trans}}$ , separating the triangular region from trapezoidal barrier.

### Resonant tunneling: A case of tip-semiconductor nanocrystal-substrate

The discrete energy levels of the conduction and valence bands of a single semiconductor NC can be measured by using STS. For single NC spectroscopy, the capping ligand coated NCs have to be deposited on atomically flat conducting substrates. Commonly, the capping molecules made of alkyl chains used to stabilize the NC size and shape. The ligand is electrically insulating. Hence, deposition of semiconductor NC on metallic substrate sets up two different insulating junctions at tip-NC ( $J_{\text{tip/NC}}$ ) and NC-substrate ( $J_{\text{NC/substrate}}$ ) respectively. It is called the double barrier tunnel junction (DBTJ) configuration (Figure 4(a)-(b)). The Fermi energy levels of tip and the substrate are located between the CB and VB gap of the NC at small bias voltages. Therefore no significant current flows through the NC at lower bias. However, at sufficient higher bias, the Fermi level of the tip or substrate becomes resonant with the CB or VB depending upon the gap between the tip and the NC. This allows electron to tunnel through the discrete energy levels of the NC. As the  $dI/dV$  spectrum directly proportional to the LDOS, the acquired tunneling characteristics reflects the CB and VB at positive and negative bias respectively.<sup>3</sup>

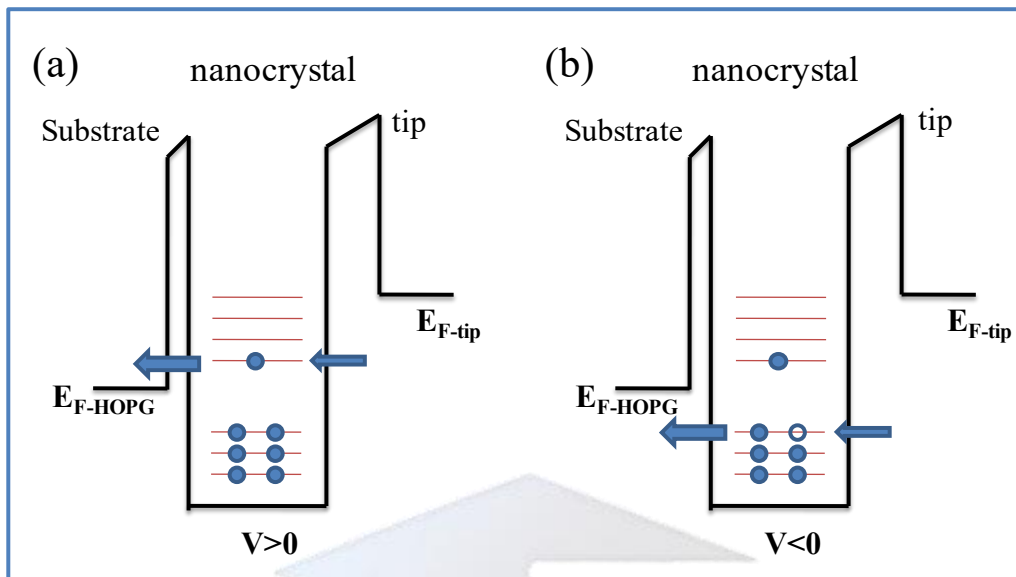


**Figure 4:** Schematic illustration of resonant tunneling mechanism at (a) positive and (b) negative bias through both conduction and valence levels.

## Experimental set up and technique of STM

Figure 5(a) shows a block diagram of a STM system, 5(b) is the Omicron UHV-STM system and 5(c) is the typical etched tip. The principle of operation of STM is based on the quantum mechanical phenomenon known as tunneling. The probability of finding tunneling electrons decreases exponentially as the distance from the surface increases. The sharp metallic tip (typically made of tungsten or platinum) is positioned a few Angstroms from the sample surface. Applying bias voltage between the tip and the surface, the wave functions of the tip atoms and the surface atoms get overlapped and causing electrons to tunnel across the gap. The STM probe can sense variations in the tunneling current across the surface. This information is processed to simulate a topographical image of the surface. The most important components of scanning tunneling microscope are:

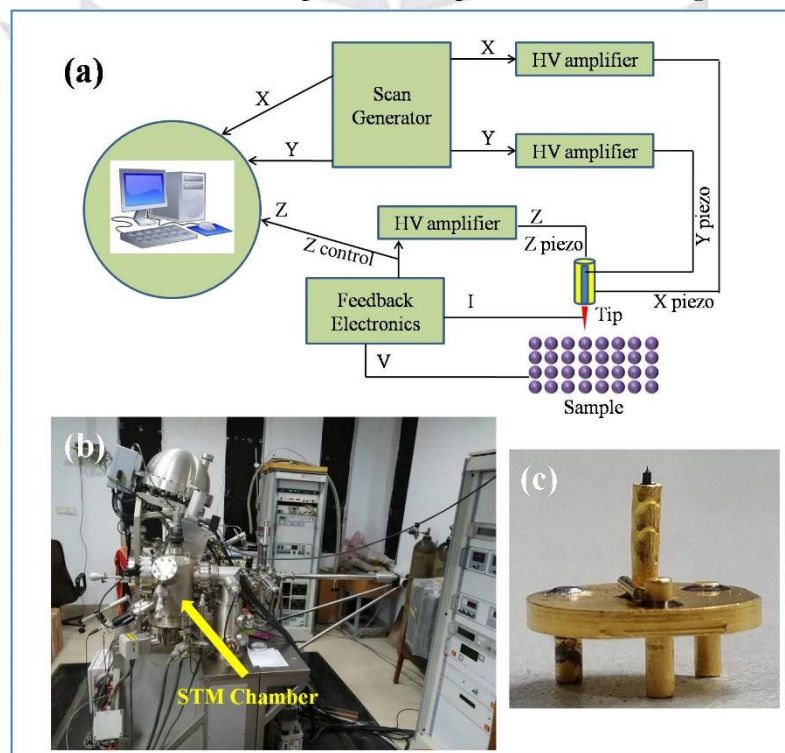


**Figure 5:** (a) Schematic diagram of STM (b) Omicron STM set up (c) Atomically sharp tip

**Atomically sharp tip:** STM tips are usually fabricated from tungsten, platinum-iridium, and gold wires (Figure 5(c)). The tip can be prepared by ex-situ as well as in-situ treatment. The ex-situ processes to make atomically sharp tip are mechanical grinding, cutting, or electrochemical etching and in-situ processes are annealing, field emission/ evaporation and even a 'soft crash' of the tip by gentle touching a sample surface. Applying high-electric-field or high-tunnelling current during scanning is very commonly used tip treatment during scanning of an image to higher resolution. However, it is very much important to avoid the double tip or asymmetric tip formation which may produce misleading sample topography.<sup>1</sup>

**Scanner:** To place the tip over the sample surface at a specific distance, a scanner is attached with the tip. A three-dimensional scanner is a piezoelectric device which can move the tip across the sample surface (x, y) and controls accurately the tip-sample separation (z). A piezoelectric actuator is an electro-mechanical device that experiences a dimensional change when an electric voltage is applied. It can convert electric signals of 1 mV to 1 kV into mechanical motion ranging from fractions of an Å to a few μm. Among several polycrystalline-piezoelectric ceramic materials, lead zirconate titanate [Pb(Ti, Zr)O<sub>3</sub>] (PZT) is widely used in the STM instrument.

**Feedback electronics:** Proper feedback electronics is also essential to operate STM at a constant current ('set-point' current). The operation is based on the principle of negative feedback, which is fed into the Z-piezoelectric driver to control the tip-sample separation gap. If the tunneling current exceeds the set-point current, the tip is pulled away from the surface by applying the appropriate signals to the Z-piezo control as well as, for a below set-point current, the tip is brought closer to the surface until the demanded tunneling current is obtained.

**Computer system:** Computer system is necessary for communication between human and the instrument. The computer provides the necessary signals for tip controlling, scanning, collecting data, storing and converting the data into an image. Two-dimensional data are typically displayed on the screen in a so-called false coloured representation, where for each (x, y)-value the measured signal is encoded by a coloured pixel. Generally, elevations in sample topography are displayed in a brighter colour than depressions. The collected data is processed for optimal contrast in display.

**Coarse-approach system:** This device is needed to move the scanner tube close to the sample within the range of the Z-piezo as per our eye permits. Such a device also needs to be able to move the sample far enough away from the tip to allow sample transfer.

**Vibration isolation system:** One of the most important parts for STM imaging is its vibration isolation system. Changes of the tip-sample separation caused by vibrations should be kept to less than ~ 0.01Å for atomically sharp imaging. There are three major parts in vibration isolation system in a common UHV-STM system, *i.e.* the outer frame structure, the springs, and the eddy current dampers. The outer frame provides a firm mounting structure that connects all components inside STM. The springs (very low spring constant) suspend the central floating platform and provide the most vibration isolation for it. Lastly, the eddy current dampers provide damping, reducing oscillations over time. Because of its vacuum compatibility and easily varied damping coefficient, eddy current dampers are the most widely used in STM instrument. Apart from this, STM is placed on a specially treated floor, made up of concrete, sand filling and compressed rubber sheet staking for minimizing the vibration.<sup>1-3</sup>

## Imaging and spectroscopic technique

STM experiment can be performed in different modes by varying the basic parameters - lateral coordinates (x, y), height (h), bias voltage (V) and tunneling current (I). In the following section we will discuss on different modes

of operation of STM: (i) constant current mode and (ii) constant height mode. Apart from these modes there is scanning tunneling spectroscopy (STS) which is rather a series of various modes where  $V$  is varied.

**Constant-Current mode:** Constant-current imaging mode is the mostly used in STM operation. The tip is scanned across the surface at a constant current. Simultaneously a feedback system adjusts the vertical position of the tip to maintain the pre-set value of the tunneling current by varying the feedback voltage  $V_z$  on the Z-piezoelectric driver, which leads to the change in tip-sample gap. For an ideal electronically homogeneous surface, constant current basically means constant gap. The height of surface features is deduced from  $V_z$ . Though the contour map  $z(x, y)$  is often referred to as the 'topographic image' of the sample surface, it is generally not solely the arrangement of atoms on a surface which determines  $z(x, y)$ . The contour map  $z(x, y)$  rather describes a constant current surface according to the experimental measurement process. This process doesn't need the surface to be atomically flat.<sup>2</sup>

**Constant-Height mode:** In this mode the tip is scanned across the surface keeping  $V_z$  constant and the fluctuation of current are registered as a function of the tip position as depicted in Figure 2.7(b). This mode scanning is faster with respect to the constant current mode scanning as the feedback loop is completely off. As a result, this mode very much useful to collect STM images at real-time video rates, which offers the opportunity to observe dynamical atomic scale processes at surfaces, e.g. surface diffusion. But, this mode of operation is useful only for relatively flat surfaces.<sup>2</sup>

**Scanning tunneling spectroscopy (STS):** Bias dependency of the tunneling current allows us to use STM as a spectroscopic tool to investigate the electronic structure of the surfaces. As the tunneling current is proportional to the LDOS of the electronic states of sample and tip, the tunneling current can be expressed in the lower-voltage limit, considering the tip to be a hemisphere with s wave function as

$$I \propto V \rho_s(r_0; E_F) \rho_t(E_F)$$

where  $\rho_s(r_0; E_F)$  is the surface/sample density of states (DOS) of the sample at the centre ( $r_0$ ) of the tip, and  $\rho_t(E_F)$  is the DOS of the tip at the Fermi level. This relationship shows that the tunneling tip follows a contour LDOS. At low voltage, states near the Fermi level only contribute to the tunneling current. For a finite bias voltage,

$$I \propto \int_0^{eV} \rho(E) D(E, V) dE$$

the tunneling current equation is modified to:

where  $\rho(E)$  is the DOS of the surface/sample and  $D(E, V)$  is the transmission coefficient of the barrier at bias voltage  $V$ . There are four spectroscopic model used in STM device: (i) current-voltage spectroscopy (ii) current-separation characteristics (iii) constant-current topography and (iv) current imaging tunneling spectroscopy (CITS). Among them Current-voltage spectroscopy is used commonly. Current-voltage spectroscopy is performed at a fixed tip-sample separation (switching off the feedback loop) by sweeping the bias voltage from a defined lower to a defined upper limit; resulting I-V is recorded and numerically differentiated. For lower voltages ( $< 1V$ ), the I-V curves show a linear voltage-dependent characteristics of Ohmic behaviour, whereas for larger voltages exponential characteristic is observed. Another STM operation mode calculates  $dI/dV$  by adding a small AC component to the DC bias voltage. The frequency should be sufficiently high so that the feedback cannot respond to it.  $dI/dV$  is measured as a function of  $V$  by sweeping  $V$ .<sup>1,3-4</sup>

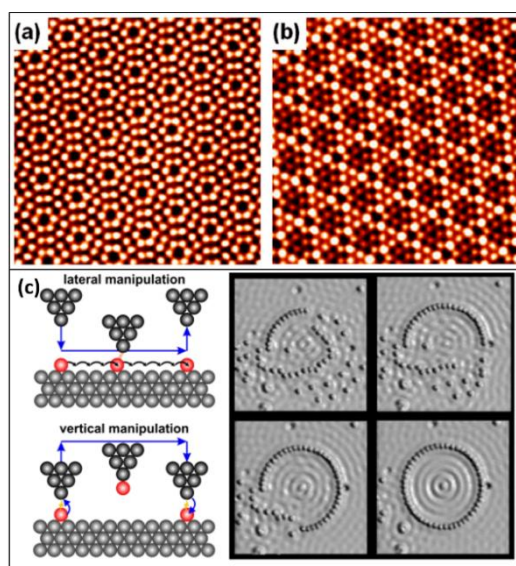


**Figure 6:** Atomic resolution of Si (111) 7x7 at (a) positive bias (b) negative bias (c) quantum atom manipulation

Along with these modes of operation, STM can be operated in manipulation mode (figure 6(c)) to move atom throughout the surface by bringing the tip into contact or near-contact to the surface. This mode of operation should be performed at cryogenic temperatures to reduce the diffusion of the adsorbate and to increase the mechanical stability of the STM. The tip is placed precisely on an atom; then, short-range forces between the tip and the atom is used to manipulate it with atomic accuracy. There are two modes of manipulation: the lateral manipulation method, where an atom is moved across the surface without losing the contact to it; and the vertical manipulation method, where the atom is picked up and then lodged at the desired position.<sup>5,6</sup> For lateral manipulation at atomic scale, the interaction forces between the tip and the surface atom, *i.e.*, Van-der-Waals or chemical forces are sufficient to move atoms, and no electric field or tunneling current is needed to be applied. However, vertical manipulation is achieved with field and current effects.<sup>6</sup>

## Data Analysis

A typical data is taken as an example from the journal<sup>7</sup> to discuss how the STM and STS data is analyzed. Figure 7(a) shows the STM image of a PbS nanorod of diameter of 5-6 nm and the corresponding height profile ( $\sim 1.7$  nm) along the length of the PbS nanorod is  $\sim 25$  nm (Figure 7(b)). A finite radius of the STM tip may contribute to the apparent enlargement of nanorod dimensions. The tunneling spectra (I-V curves) were collected at three different positions on an isolated nanorod by keeping the set-current (0.1 nA) and set-voltage (1 V) constant while disabling the feed-back controls. The I-V curves measured at three different positions on PbS nanorod reveal semiconductor behavior on either side of the zero bias voltage (Figure 7(c)). The magnitude of current is observed to be similar for three different locations of the nanorod. Corresponding  $(dI/dV)/(I/V)$  spectra at three different positions along the PbS nanorod, which are the replica of local density of states (LDOS) at corresponding positions, are calculated by numerical differentiation of I-V curves (Figure 7(d)). Zero-conductivity region in a  $(dI/dV)/(I/V)$  curve, which is in direct correlation with band gap of the material, is observed to be constant for all the three different positions of PbS nanorod. It is well established that these  $dI/dV$  spectra of a single NC reflects the peak like behavior corresponding to the conduction and valence levels at positive and negative bias, respectively. Corresponding tunneling mechanism through the single NC suggests the resonant tunneling of electrons under double barrier tunnel junction (DBTJ) mechanism. Our  $dI/dV$  spectra indeed reflect the peak like behavior on either side of the zero bias voltage, from which we have extracted the conduction band (CB) or valence band (VB) positions of PbS nanorod. Corresponding threshold positions for

the CB ( $\sim 0.65$  V) and VB ( $\sim 0.4$  V) are also observed to be the same along the nanorod indicating that no considerable deviation in the electronic structure occurs along the length of the nanorod. From the difference in the threshold positions for the CB and VB, we have calculated the tunneling band gap for the PbS nanorod to be 1.05 eV.<sup>7</sup>

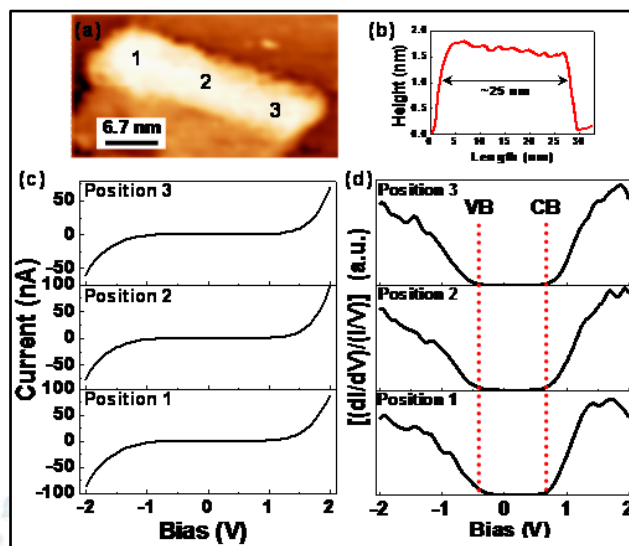


**Figure 7:** (a) STM image of PbS nanorod (b) Line profile of PbS nanorod (c) STS (I-V) taken at 3 different points mentioned in figure 6(a) (d)  $(dI/dV)/(I/V)$  of that mentioned 3 points

## Applications of Scanning Tunneling Microscope:

The Scanning Tunneling Microscope has proven to be an invaluable tool in various scientific and technological fields:

**Surface Imaging:** STM enables scientists to visualize the atomic arrangement on the surface of conductive materials. It has been particularly useful in studying crystals, semiconductor surfaces, and nanostructures.

**Manipulation of Atoms:** With the help of STM, individual atoms and molecules can be manipulated and moved on the surface with exceptional precision. This opens up possibilities for creating nanostructures and exploring nanotechnology.

**Surface Analysis:** STM can be utilized to investigate the electronic properties of surfaces and analyze the local density of states. This information is vital for understanding material behavior and surface reactivity.

**Nanotechnology:** STM has been an essential instrument in advancing nanotechnology research. It allows scientists to engineer and study nanoscale devices and materials, which are crucial in developing future technologies.

**Biological Sciences:** While STM primarily works with conductive samples, variants like the Atomic Force Microscope (AFM) have been developed to study non-conductive materials, including biological samples like proteins and DNA molecules.

## Conclusion:

The scanning tunneling microscope has firmly established itself as one of the most transformative instruments in modern science, offering an unprecedented window into the atomic landscape of materials. By harnessing the quantum tunneling effect, it allows researchers to visualize, characterize, and even manipulate individual atoms with extraordinary precision—capabilities that were unimaginable before its invention. Its influence extends far beyond surface imaging, contributing significantly to the growth of nanoscience, quantum research, and materials engineering. The STM's ability to probe electronic properties at the nanoscale has advanced

our understanding of phenomena such as superconductivity, magnetism, and molecular interactions. As both a scientific tool and a technological milestone, the scanning tunneling microscope continues to shape the future of nanoscale exploration, driving innovations that deepen our comprehension of matter at its smallest dimensions.

## Referances

- Wiesendanger, R. (1994). *Scanning Probe Microscopy and Spectroscopy*. Cambridge University Press.
- Binnig, G., & Rohrer, H. (1983). Scanning tunneling microscopy. *Surface Science*, 126(1-3), 236–244. [https://doi.org/10.1016/0039-6028\(83\)90716-1](https://doi.org/10.1016/0039-6028(83)90716-1)
- C Julian Chen. (2021). *Introduction to scanning tunneling microscopy*. Oxford Oxford University Press.
- Khajetoorians, A. A., Wegner, D., Otte, A. F., & Swart, I. (2019). Creating designer quantum states of matter atom-by-atom. *Nature Reviews Physics*, 1(12), 703–715. <https://doi.org/10.1038/s42254-019-0108-5>
- Guo, H., Wang, Y., Du, S., & Gao, H. (2014). High-resolution scanning tunneling microscopy imaging of Si (1 1 1)-7 × 7 structure and intrinsic molecular states. *Journal of Physics: Condensed Matter*, 26(39), 394001. <https://doi.org/10.1088/0953-8984/26/39/394001>
- Barberán, J. R. M. (2024). Scanning Tunneling Microscopy: A Review. *Nanotechnology Perceptions*, 1994–2006. <https://doi.org/10.62441/nano-ntp.vi.3063>
- Debangshi, A., Thupakula, U., Khan, A. H., Kumar, G. S., Sarkar, P. K., & Acharya, S. (2018). Probing Local Electronic Structures of Au–PbS Metal–Semiconductor Nanodumbbells. *ACS Applied Nano Materials*, 1(5), 2104–2111. <https://doi.org/10.1021/acsanm.8b00097>

